Biochimica et Biophysica Acta 1842 (2014) 1844–1854

Contents lists available at ScienceDirect

Biochimica et Biophysica Acta

journal homepage: www.elsevier.com/locate/bbadis

AMPK activation prevents excess nutrient-induced hepatic lipid accumulation by inhibiting mTORC1 signaling and endoplasmic reticulum stress response

Hongliang Li, Qing Min, Changhan Ouyang, Jiyeon Lee, Chaoyong He, Ming-Hui Zou, Zhonglin Xie *

Section of Molecular Medicine, Department of Medicine, University of Oklahoma Health Sciences Center, Oklahoma City, OK 73104, USA

ARTICLE INFO

Article history:
Received 2 April 2014
Received in revised form 1 July 2014
Accepted 2 July 2014
Available online 10 July 2014

Keywords:
AMPK
ER stress
mTORC1
SREBP
Lipid accumulation

ABSTRACT

Lipid accumulation is a central event in the development of chronic metabolic diseases, including obesity and type 2 diabetes, but the mechanisms responsible for lipid accumulation are incompletely understood. This study was designed to investigate the mechanisms for excess nutrient-induced lipid accumulation and whether activation of AMP-activated protein kinase (AMPK) prevents the hepatic lipid accumulation in excess nutrient-treated HepG2 cells and high fat diet (HFD)-fed mice. Exposure of HepG2 cells to high levels of glucose or palmitate induced the endoplasmic reticulum (ER) stress response, activated sterol regulatory element-binding protein-1 (SREBP-1), and enhanced lipid accumulation, all of which were sensitive to ER stress inhibitor and gene silencing of eukaryotic initiation factor 2α. The increases in ER stress response and lipid accumulation were associated with activation of mammalian target of rapamycin complex 1 (mTORC1) signaling. Inhibition of mTORC1 signaling attenuated the ER stress response and lipid accumulation induced by high glucose or by deletion of tuberous sclerosis 2. In addition, AMPK activation prevented the mTORC1 activation, ER stress response, and lipid accumulation. This effect was mimicked or abrogated, respectively, by overexpression of constitutively active and dominant-negative AMPK mutants. Finally, treatment of HFD-fed mice with 5-aminoimidazole-4-carboxamide-1-β-4-ribofuranoside inhibited the mTORC1 pathway, suppressed the ER stress response, and prevented insulin resistance and hepatic lipid accumulation. We conclude that activation of AMPK prevents excess nutrient-induced hepatic lipid accumulation by inhibiting mTORC1 and ER stress response.

1. Introduction

Nutrient overload is a major cause of chronic metabolic diseases, including obesity, diabetes, and cardiovascular disease. Excessive intake of nutrients (lipids, proteins, and carbohydrates) causes lipid accumulation in fat tissue, skeletal muscle, and the liver, leading to insulin resistance and metabolic disorders [1]. Lipid metabolism occurs mainly at the endoplasmic reticulum (ER), where many of the enzymes related to lipid metabolism reside [1]. The ER is a highly dynamic organelle and plays an important role in maintaining metabolic homeostasis. When the ER is challenged, the ER stress is activated and the unfolded protein response (UPR) is initiated through three ER membrane proteins: inositol-requiring enzyme 1, activating transcription factor-6 (ATF6), and protein kinase-like ER kinase (PERK). Disruption of the ER stress response has been implicated in the development of obesity, diabetes, and atherosclerosis [2]. In pancreatic β cells, the activation of PERK and eukaryotic translation initiation factor 2 subunit alpha (eIF2α) upregulates the expression of sterol regulatory element-binding proteins (SREBPs), which are major regulators of cholesterol and fatty acid synthesis [3]. In mammary epithelial cells, the loss of PERK reduces SREBP activity and lipogenesis [4]. Thus, the ER stress response may be a mechanistic link between excess nutrients and lipid accumulation, which is a crucial event in the development of metabolic syndrome.

The mammalian target of rapamycin (mTOR), a coordinator between nutritional stress and cellular growth machinery, is associated with the pathogenesis of insulin resistance. Nutrient overload induces constitutive p70 ribosomal S6 kinase (S6K) activation, which leads to insulin resistance by suppressing insulin-induced class I PI3K (phosphoinositide 3-kinase) signaling [5]. The mTOR exists as two distinct protein complexes, mTOR complex1 (mTORC1) and mTOR complex2 (mTORC2) [6–9]. Activation of mTORC1 increases protein synthesis and ribosomal biogenesis, thereby playing a key role in coupling nutrients to growth [10]. Activation of mTORC1 also regulates the expression of hepatic SREBP-1c and lipogenesis [11,12]. Moreover, activation of mTORC1 by deletion of TSC1 or TSC2 has been shown to

* Corresponding author at: Section of Molecular Medicine, Department of Medicine, University of Oklahoma Health Sciences Center, 941 Stanton L. Young Blvd. BSEB 302B, Oklahoma City, OK 73104, USA. Tel.: +1 405 271 3077; fax: +1 405 271 3973.
E-mail address: zxie@ouhsc.edu (Z. Xie).

http://dx.doi.org/10.1016/j.bbadis.2014.07.002
0925-4439/

activate the ER stress response [13]. These findings lead us to hypothesize that activation of mTORC1 may mediate excess nutrient-induced ER stress and intracellular lipid accumulation.

The AMP-activated protein kinase (AMPK) senses intracellular energy status [14] and plays an important role in the regulation of glucose and lipid metabolism [15]. Activation of AMPK phosphorylates several target molecules, resulting in the downregulation of anabolic pathways to conserve ATP and the upregulation of catabolic pathways to generate more ATP [16]. Activation of AMPK provides an important cellular protective response to various stress conditions, including hypoxia [17], oxidative stress [18,19], exercise [20], and starvation [21].

In the diabetic hearts AMPK activation has been shown to restore autophagy, inhibit cardiomyocyte apoptosis, and improve cardiac function [22–26]. In addition, several studies suggest that activation of AMPK protects against hypoxia-induced cardiomyocyte apoptosis, and reduces atherosclerosis by suppressing the ER stress response [2,17]. However, whether AMPK activation prevents excess nutrient-induced hepatic lipid accumulation through inhibition of the ER stress response remains unknown. The present study was designed to elucidate the mechanism by which excessive intake of nutrients results in hepatic lipid accumulation, and to determine the role of AMPK in preventing excess nutrient-induced hepatic lipid accumulation. Our data suggest that excess nutrients activate mTORC1 signaling, which induces the ER stress response and subsequent hepatic lipid accumulation. Activation of AMPK prevents hepatic lipid accumulation by suppressing the mTORC1-ER stress pathway.

2. Materials and methods

2.1. Reagents

Human hepatocarcinoma HepG2 cells were obtained from Cascade Biologics (Portland, OR). Dulbecco's modified Eagle's medium (DMEM) was purchased from Mediatech, Inc. (Herndon, VA). Fetal bovine serum (FBS) was obtained from Invitrogen Corporation (Carlsbad, CA). The following antibodies were purchased from Cell Signaling Technology (Beverly, MA): phosphor-mTOR (Ser2448), phosphor-AMPK (Thr172), AMPK-α, phosphor-S6K (Thr389), SREBP-1, fatty acid synthase (FAS), Ras homolog enriched in brain (Rheb), 78 kDa glucose-regulated protein (GRP78), phosphor-PERK, phosphor-eIF2α, eukaryotic translation initiation factor 4E binding protein 1 (4EBP1), and phosphor-4EBP-1 (Thr37/46). The antibody against β-actin was acquired from Santa Cruz Biotechnology (Santa Cruz, CA). All secondary antibodies were obtained from Jackson ImmunoResearch Laboratories, Inc. (West Grove, PA). AICAR (5-aminoimidazole-4-carboxyamide ribonucleoside) was procured from Toronto Research Chemicals, Inc. Compound C and rapamycin were purchased from Calbiochem (San Diego, CA). Tunicamycin, 4-phenyl butyric acid (PBA), palmitate, human recombinant insulin, and other chemicals were obtained from Sigma.

2.2. Experimental animals

The animal protocol was reviewed and approved by the University of Oklahoma Institutional Animal Care and Use Committee. At 12 weeks of age, male C57BL/6J mice (Jackson Laboratories, Bar Harbor, MI) were fed either a normal diet (ND; 20% protein, 70% carbohydrate, 10% fat) or a high fat diet (HFD; 20% protein, 35% carbohydrate, 45% fat, total 5.7 kcal/g). Both diets were obtained from Research Diet, Inc., New Brunswick, NJ (ND: D12450B, HFD: D12451). At the same time, the mice were randomly assigned to receive intraperitoneal injections of AICAR (250 mg/kg/day) or vehicle. After 2 months of treatment, the animals were euthanized and livers were collected for biochemical and molecular biological analyses.

2.3. Cell culture and treatment

HepG2 cells were maintained in DMEM with 1 g/L glucose containing 10% fetal bovine serum. TSC2 deletion ($TSC2^{-/-}$) mouse embryotic fibroblasts (MEFs) provided by Brendan Manning and David Kwitakowski (Harvard Medical School) were cultured in DMEM with 10% fetal bovine serum. All culture media were supplemented with penicillin (100 U/mL) and streptomycin (100 μg). The cells were incubated in a humidified atmosphere of 5% CO_2 and 95% air at 37 °C.

2.4. Adenovirus infection and gene silencing of eIF2α

The constitutively active AMPK adenoviral vector (CA-AMPK) was constructed from a rat cDNA encoding residues 1–312 of AMPKα1, in which Thr172 was mutated into aspartic acid (T172D). The dominant-negative AMPK adenoviral vector (DN-AMPK) was constructed from AMPKα2 bearing a mutation altering lysine 45 to arginine (K45R), as described previously [27]. Adenovirus encoding green fluorescent protein (GFP) served as a control. HepG2 cells were infected with the indicated adenovirus at an MOI of 50 in serum-free medium overnight. The cells were then washed and incubated in fresh serum-free medium for an additional 18–24 h before use in the experiments. Under these conditions, infection efficiency was typically >80%, as determined by measuring GFP expression [19,28]. Scrambled siRNA and eIF2α-specific siRNA were obtained from Applied Biosystems (Foster City, CA). Transfection was performed according to the manufacturer's instructions. The efficiency of siRNA transfection was evaluated by Western blotting of eIF2α with a specific antibody.

2.5. Hyperinsulinemic–euglycemic clamp

The hyperinsulinemic–euglycemic clamps were performed as described previously [29,30]. Briefly, mice were anesthetized by intraperitoneal injection of ketamine (100 mg/kg) and xylazine (20 mg/kg). Heparin (200 U/mL) was intraperitoneally injected to prevent blood clotting. A polyethylene catheter was inserted into the right jugular vein for infusion of 20% glucose and insulin (2 mU/mL) in normal saline, using a peristaltic pump. The left carotid artery was cannulated for blood sampling. Insulin (3 mU/kg/min) was infused through the jugular vein catheter from 0 to 120 min. During this period, the blood glucose concentration was monitored every 5 min with a glucometer and clamped at euglycemic levels (5.0 ± 0.5 mmol/L) by a variable infusion of 20% glucose. Clamping was achieved by 90 min and maintained for 30 min. The mean glucose infusion rates (ml/min/kg) were calculated during the last 30 min of the clamp. To determine blood glucose levels, mice were fasted overnight and their blood glucose was monitored by applying tail blood to the glucometer.

2.6. Measurement of intracellular lipid, cholesterol, and triglyceride contents

The intracellular lipid contents of cultured HepG2 cells were evaluated by Oil Red O staining. Briefly, the cells were fixed in 4% paraformaldehyde in PBS for 30 min, stained with Oil Red O for 1 h at room temperature, and then rinsed with water. Lipids in cultured HepG2 cells and mouse liver were extracted as described by Folch et al. [31]. Cholesterol and triglyceride levels in extracted lipids were measured enzymatically using the reagents from Cayman Chemical (Ann Arbor, MI) according to the manufacturer's instruction.

2.7. Western blot analysis

We extracted proteins from cultured cells and mouse livers, and subjected cell lysates to Western blot analysis as described previously [19,28]. The protein content was assayed by BCA protein assay reagent (Pierce, Rockford, IL). The lysates were resolved by SDS-PAGE and

then transferred to a nitrocellulose membrane. We incubated the membrane with a 1:1000 dilution of primary antibodies, followed by a 1:5000 dilution of horseradish peroxidase-conjugated secondary antibodies. Nuclear fractions were prepared as described previously [19]. The protein levels of SREBP-1 were determined by Western blotting. The signal was revealed using chemiluminescence. We quantified the optical density of bands using the AlphaEase (Alpha Innotech Corporation) image system and expressed it as arbitrary units [32,33].

2.8. RNA extraction and quantitative real-time PCR (QRT-PCR)

We extracted the total mRNA from cultured cells and livers with Trizol reagent (Invitrogen). For reverse transcription, 1 μg of the total mRNA was converted to first strand complementary DNA in 20 μL reactions using a cDNA synthesis Kit (Promega). Quantitative RT-PCR reactions were performed as described previously [34,35]. Calculations were performed by a comparative method ($2^{-\Delta\Delta}$Ct) using GAPDH as an internal control [36]. The primers used for the PCR are as follows: fatty acid synthase (FAS): forward 5′-AGGGGTCGACCTGGTCCTCA-3′, reverse 5′-GCCATGCCCAGAGGGTGGTT-3′; acetyl CoA carboxylase (ACC-1): forward 5′-CGAAAGACTCTTAACTCTGG-3′, reverse 5′-CCAG GTTACTGATCTCATCT-3′; ATP citrate lyase (ACLY): forward 5′-GTCAGC CAAGGCAATTTCAGAG-3′, reverse 5′-TAACCCGGGCATACTTGAACC-3′; sterol CoA desaturase-1 (SCD1): forward 5′-ACACCCGGCTGTCAAAGA GA-3′, reverse 5′- GGAGGCCAGGCTTGTAGTACCT-3′.

2.9. Statistics

Data are expressed as mean ± standard errors of the mean (*SEM*). Statistical analyses were performed with the Student's *t*-test (2 groups) or one-way ANOVA with the Bonferroni procedure for multiple comparison tests (≥3 groups). $P < 0.05$ was considered statistically significant.

3. Results

3.1. Elevated glucose levels stimulate ER stress, activate SREBP-1, and increase lipid accumulation in HepG2 cells

SREBPs are a family of transcription factors that regulate the lipid metabolic genes related to fatty acid and cholesterol biosynthesis [37,38]. SREBP-1 processing has been reported to be regulated through the PERK–eIF2α pathway [4]. To determine the mechanism underlying

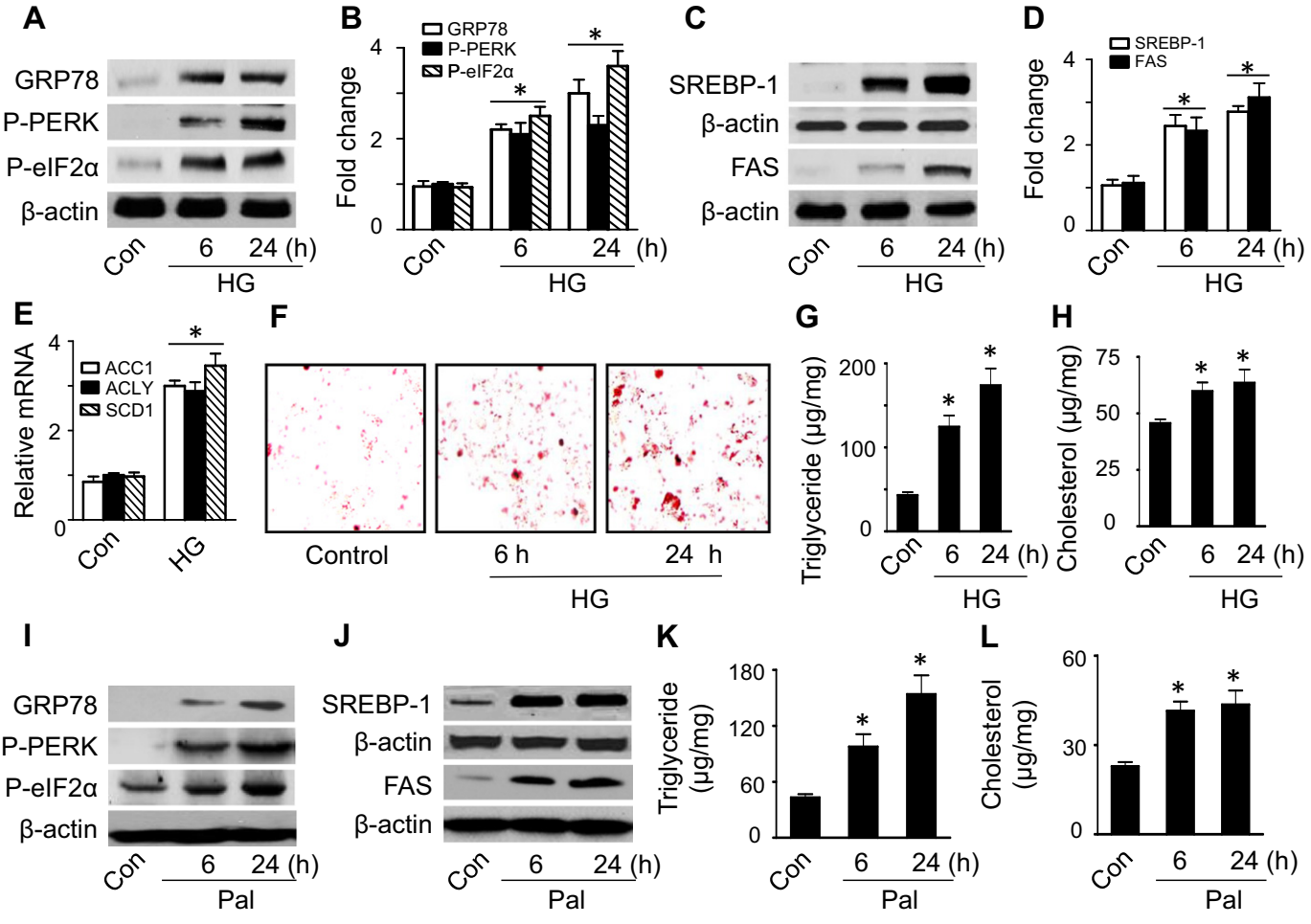

Fig. 1. High glucose and palmitate induce ER stress and lipid accumulation. (A–H) HepG2 cells were incubated in the presence or absence of high glucose (HG, 30 mM) for the indicated time. Levels of GRP78, P-PERK, and P-eIF2α (A and B) were analyzed by Western blotting and quantified by densitometry. *, $P < 0.05$ vs. control (Con); $n = 5$. (C and D) Protein levels of SREBP-1 in the nuclear fractions and FAS in cell lysates were analyzed by Western blotting and quantified by densitometry. *, $P < 0.05$ vs. control (Con); $n = 5$. (E) Relative levels of ACC1, ACLY, and SCD1 mRNA were determined by RT-PCR. *, $P < 0.05$ vs. Con; $n = 3$. (F) Lipid accumulation was determined by Oil red O staining. Images are representative of results of three independent experiments. Lipids were extracted and triglyceride (G) and cholesterol (H) levels were measured using a commercial kit. *, $P < 0.05$ vs. Con; $n = 5$. (I–L) HepG2 cells were incubated in the presence or absence of 0.4 mM palmitate (Pal) for indicated time. (I) Levels of ER stress markers GRP78, P-PERK, and P-eIF2α were determined by Western blotting. (J) Levels of SREBP-1 in the nuclear fractions and FAS in cell lysates were determined by Western blotting. Blots are representative of three independent experiments. Concentrations of triglyceride (K) and cholesterol (L) were assayed using a commercial kit. *, $P < 0.05$ vs. Con; $n = 5$. Values are expressed as mean ± standard errors of the mean (*SEM*).

nutrient-induced hepatic lipid accumulation, we exposed HepG2 cells to high glucose for 6 or 24 h, and then examined the cells' ER stress response, SREBP-1 activation, and lipid contents. Elevated glucose levels stimulated ER stress in a time-dependent manner, as indicated by increased expression of GRP78 and phosphorylation of PERK and eIF2α (Fig. 1A and B). This was not due to the increase in osmolarity, because incubation of HepG2 cells with 25 mM mannitol plus 5 mM glucose had no effect on the ER stress response (data not shown). To assess SREBP-1 activation, we detected the expression of the cleaved, mature 68 kDa form of SREBP-1 in the nuclear fractions by Western blotting. The cells treated with high glucose exhibited higher levels of cleaved SREBP-1 in the nuclear fractions (Fig. 1C and D) than the control cells. The activation of SREBP-1 was associated with increases in its target genes, including ACC1, ACLY, and SCD1 (Fig. 1E), and upregulation of FAS protein levels (Fig. 1C and D). Concomitantly, high glucose treatment resulted in lipid accumulation in the cells. Oil red O staining revealed a clear increase in total lipid levels in the cells (Fig. 1F). Because plentiful extracellular lipids may mask intracellular lipid staining, lipid content was further measured enzymatically using a commercial kit. The analysis revealed significant increases in intracellular triglyceride and cholesterol levels (Fig. 1G and H). These results suggest that elevated glucose levels were associated with the activation of the ER stress response and the increase in intracellular lipid accumulation.

3.2. Palmitate induces ER stress and intracellular lipid accumulation

We further incubated HepG2 cells in medium containing palmitate to mimic fatty acid overload conditions. Similar to the aforementioned results with elevated glucose, palmitate also increased the expression of ER stress markers, such as GRP78, P-PERK, and P-eIF2α (Fig. 1I), activated SREBP-1 (Fig. 1J), upregulated FAS (Fig. 1J), and induced lipid accumulation, as evidenced by high intracellular levels of triglycerides (Fig. 1K) and cholesterol (Fig. 1L). Taken together, our results indicate that nutrient overload stimulated ER stress and induced intracellular lipid accumulation. Because elevated glucose and/or fatty acid levels have similar effects on ER stress and lipid accumulation, we used high glucose as an ER stress stimulus to determine the mechanisms involved in excess nutrient-induced lipid accumulation in the *in vitro* study.

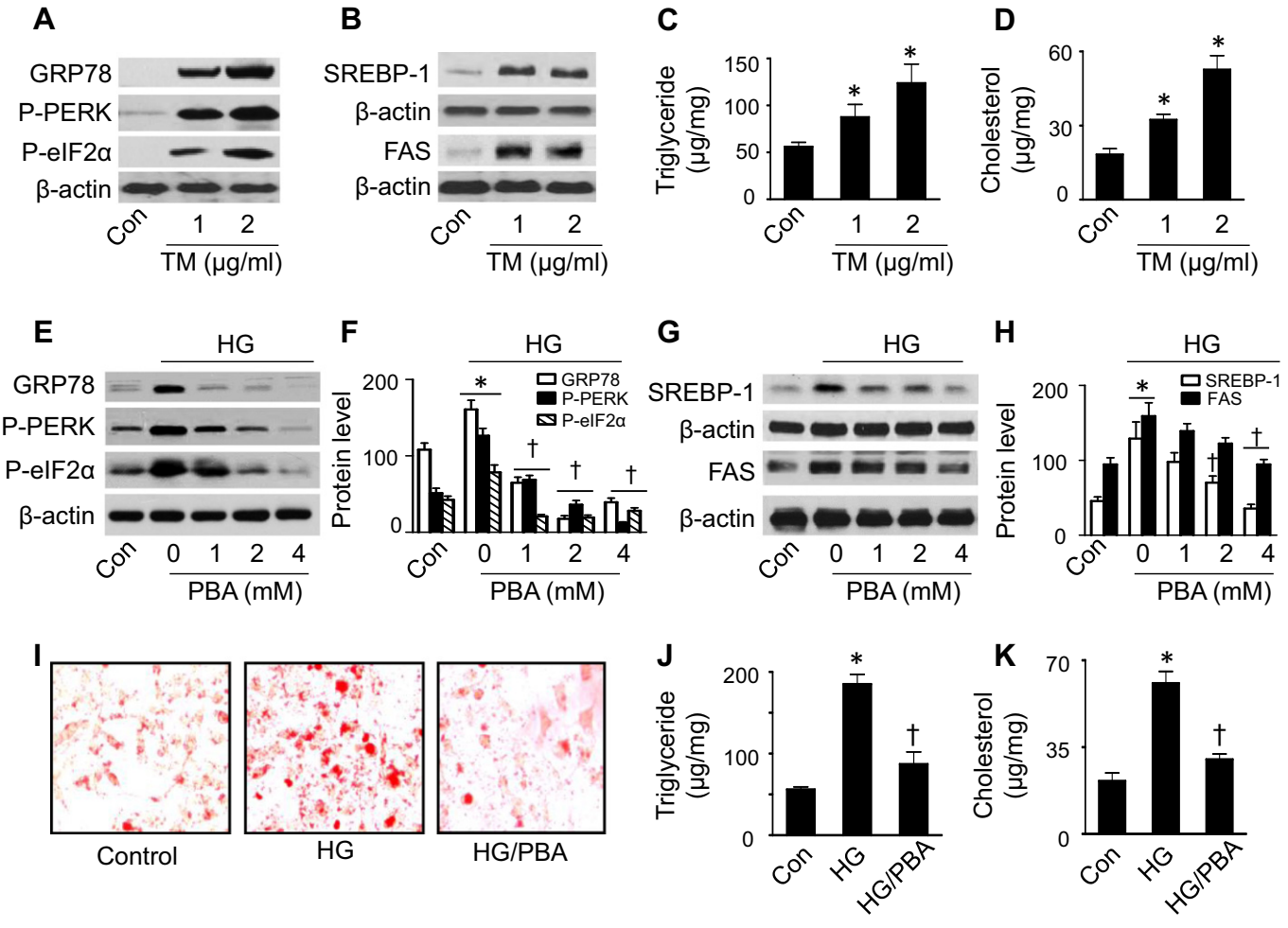

Fig. 2. Inhibition of ER stress abrogates high glucose-induced lipid accumulation. (A–D) HepG2 cells were incubated in the presence or absence of the indicated concentrations of tunicamycin (TM) for 24 h. (A) Expression of ER stress markers GRP78, P-PERK, and P-eIF2α was determined by Western analysis. (B) Expression of SREBP-1 in the nuclear fractions and FAS in cell lysates was determined by Western analysis. Blots are representative of at least three independent experiments. Triglyceride (C) and cholesterol (D) levels were measured using a commercial kit. *, $P < 0.05$ vs. Con; $n = 5$. (E–H) HepG2 cells were treated with HG in the presence or absence of the indicated concentrations of PBA. (E and F) Levels of ER stress markers were analyzed by Western blotting and quantified by densitometry. *, $P < 0.05$ vs. Con; †, $P < 0.05$ vs. HG; $n = 5$. (G and H) Levels of SREBP-1 in the nuclear fractions and FAS in cell lysates were analyzed by Western blotting and quantified by densitometry. *, $P < 0.05$ vs. Con; †, $P < 0.05$ vs. HG; $n = 5$. (I–K) HepG2 cells were incubated in the presence or absence of HG and PBA (4 mM). (I) Lipid accumulation was measured by staining with Oil red O. Images are representative of results of three independent experiments. (J and K) Triglyceride (J) and cholesterol (K) levels were measured using a commercial kit. *, $P < 0.05$ vs. Con; †, $P < 0.05$ vs. HG; $n = 5$. Values are expressed as mean ± *SEM*.

3.3. Elevated glucose levels induce lipid accumulation through activation of ER stress response

To establish the role of ER stress in lipid accumulation, we treated HepG2 cells with various concentrations of tunicamycin (TM), an ER-stress inducible reagent, for 24 h, and then analyzed the intracellular lipid contents. Consistent with the previous findings [39], tunicamycin stimulated ER stress, i.e., increased GRP78 expression, as well as PERK and eIF2α phosphorylation (Fig. 2A). At the same time, tunicamycin enhanced protein levels of SREBP-1 in the nuclear fractions (Fig. 2B), upregulated FAS protein expression (Fig. 2B), and increased intracellular triglyceride (Fig. 2C) and cholesterol levels (Fig. 2D).

Next, we investigated whether small molecule chemical chaperone 4-phenyl butyric acid (PBA), a well-characterized ER stress inhibitor [40], could alleviate the ER stress response and lipid accumulation induced by high glucose levels. Pretreatment of HepG2 cells with PBA dose-dependently reduced PERK and eIF2α phosphorylation and downregulated GRP78 expression upon exposure to elevated glucose levels (Fig. 2E and F). Under these conditions, high glucose-enhanced nuclear SREBP-1 protein levels and FAS expression were significantly attenuated (Fig. 2G and H). High glucose-enhanced intracellular lipid accumulation was also diminished, as reflected by reduced Oil red O staining (Fig. 2I) and low intracellular triglyceride (Fig. 2J) and cholesterol (Fig. 2K) levels. These data suggest that elevated glucose levels induce intracellular lipid accumulation by evoking the ER stress response.

3.4. Knockdown of eIF2α prevents high glucose-enhanced nuclear SERBP-1 levels and intracellular lipid accumulation

The PERK–eIF2α pathway has been reported to regulate SREBP-1 [4]. We therefore used a gene silencing approach targeting eIF2α to establish the role of the ER stress response in mediating high glucose-enhanced intracellular lipid accumulation. As depicted in Fig. 3A, eIF2α siRNA significantly reduced eIF2α protein levels, whereas control siRNA did not. The reduction of eIF2α expression prevented high glucose-enhanced SREBP-1 in the nuclear fractions and abolished high glucose-induced upregulation of FAS protein levels (Fig. 3A and B). Silencing eIF2α also abrogated the elevated glucose-mediated increase in triglyceride and cholesterol levels (Fig. 3C and D). Thus, activation of ER stress response is a central event in high glucose-induced intracellular lipid accumulation.

3.5. Activation of mTORC1 signaling is required for high glucose-induced ER stress

mTOR is an essential signaling pathway that senses intracellular nutritional status [41]. We therefore studied whether mTOR mediates ER stress in the presence of high glucose. Incubating HepG2 cells in elevated levels of glucose activated the mTORC1 signaling pathway, as determined by phosphorylation of mTOR at Ser2448 and its downstream effector S6K at Thr389 and 4EBP1 at Thr37 (Fig. 4A). Since Ras homolog enriched in brain (Rheb) plays critical roles in the activation of mTOR, we determined whether Rheb mediates high glucose-activated mTOR signaling by gene silencing of Rheb. Transfection of Rheb siRNA into HepG2 cells significantly reduced Rheb protein levels (Fig. 4B). In the cells transfected with control siRNA, elevated glucose concentration increased Rheb expression and concomitantly increased phosphorylation of mTOR and S6K (Fig. 4B). However, the activation of mTORC1 signaling was absent in the cell transfected with Rheb siRNA (Fig. 4B). We next examined whether inhibition of mTORC1 signaling can prevent high glucose-induced hepatic lipid accumulation. Administration of the mTORC1-specific inhibitor rapamycin suppressed the phosphorylation of mTOR, S6K, and

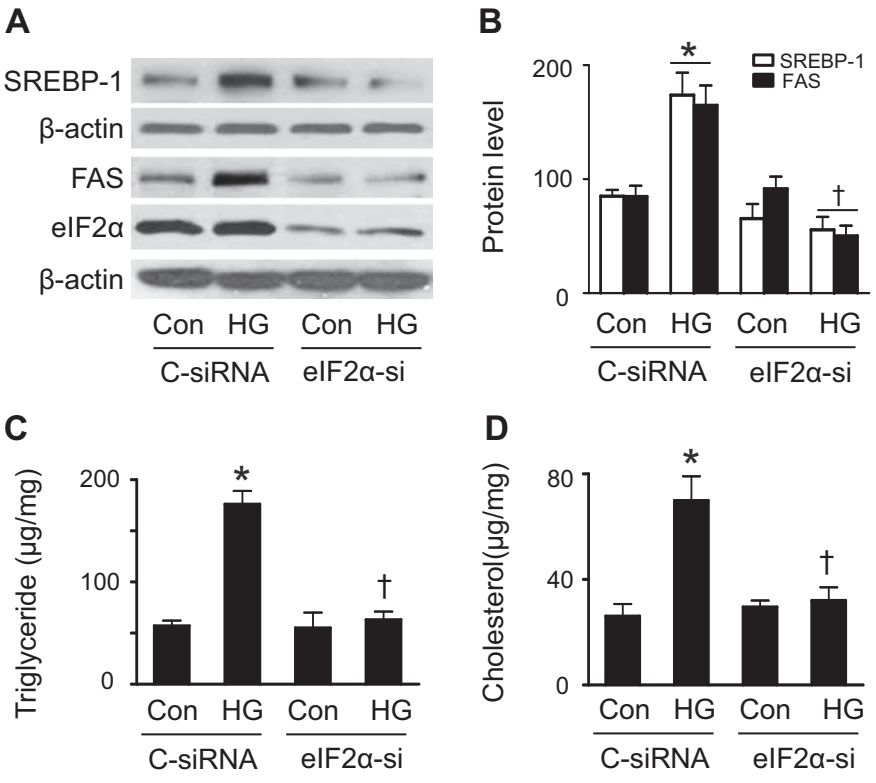

Fig. 3. eIF2α mediates high glucose-induced lipid accumulation. HepG2 cells were transfected with control (C-siRNA) or eIF2α siRNA (eIF2α-si) for 24 h, and then cultured in the presence or absence of HG for 24 h. Expression of SREBP-1 in the nuclear fractions and levels of eIF2α and FAS in the cell lysates were examined by Western analysis (A) and quantified by densitometry (B). Concentrations of triglyceride (C) and cholesterol (D) were assayed using a commercial kit. *, $P < 0.05$ vs. Con; †, $P < 0.05$ vs. C-siRNA/HG; $n = 5$. Values are expressed as mean ± *SEM*.

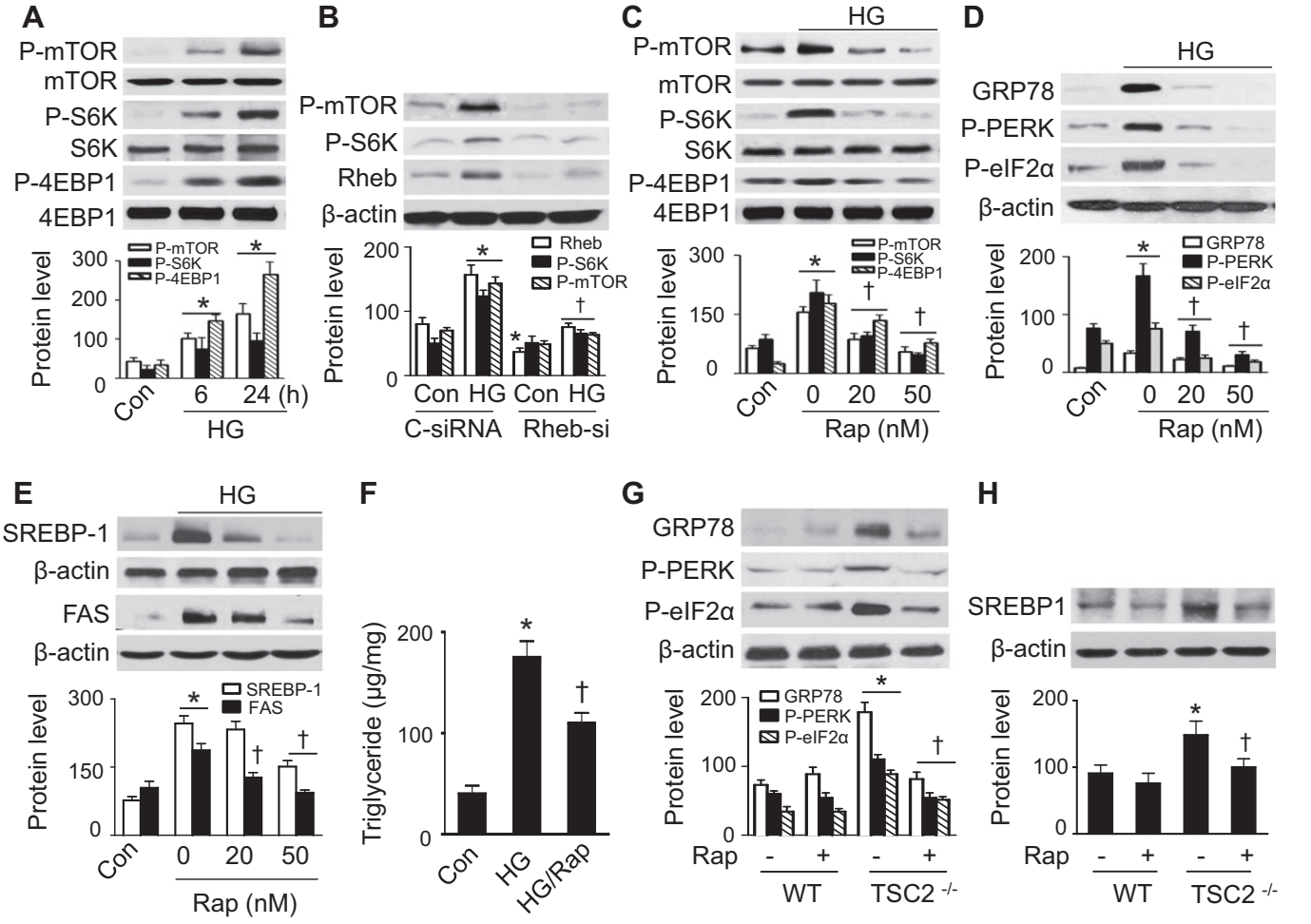

Fig. 4. Inhibition of mTORC1 signaling prevents high glucose-induced ER stress and lipid accumulation. (A) HepG2 cells were incubated in the presence or absence of high glucose (HG, 30 mM) for the indicated time. Phosphorylation of mTOR at Ser2448, of S6K at Thr389, and of 4EBP1 at Thr37 was determined by Western analysis and quantified by densitometry. *, $P < 0.05$ vs. Con; $n = 5$. (B) HepG2 cells were transfected with control (C-siRNA) or Rheb siRNA (Rheb-si) for 24 h, and then cultured in the presence or absence of high glucose for 24 h. Expression of Rheb, P-mTOR, and P-S6K in cell lysates was examined by Western blotting and quantified by densitometry. *, $P < 0.05$ vs. C-siRNA; †, $P < 0.05$ vs. HG/C-siRNA; $n = 4$. (C) HepG2 cells were pretreated with rapamycin (Rap) at the indicated concentrations and then exposed to HG for 24 h. Phosphorylation of mTOR, S6K, and 4EBP1 was examined by Western blotting. *, $P < 0.05$ vs. Con; †, $P < 0.05$ vs. HG; $n = 5$. (D and E) HepG2 cells were pretreated with rapamycin (Rap) at the indicated concentrations and then incubated in the presence of HG for 24 h. Levels of ER stress markers GRP78, P-PERK, and P-eIF2α (D) were examined by Western analysis and quantified by densitometry. *, $P < 0.05$ vs. Con; †, $P < 0.05$ vs. HG; $n = 5$. (E) Levels of SREBP-1 in the nuclear fractions and FAS in cell lysates were examined by Western analysis and quantified by densitometry. *, $P < 0.05$ vs. Con; †, $P < 0.05$ vs. HG; $n = 5$. (F) HepG2 cells were pretreated with Rap and incubated in the presence of HG for 24 h. Triglyceride concentration was measured using a commercial kit. *, $P < 0.05$ vs. Con; †, $P < 0.05$ vs. HG; $n = 5$. (G and H) Wild-type (WT) and TSC2$^{-/-}$ MEFs were incubated in the presence or absence of 50 nM Rap for 24 h. Levels of ER stress markers (G) were determined by Western analysis and quantified by densitometry. *, $P < 0.05$ vs. Con; †, $P < 0.05$ vs. TSC2$^{-/-}$ control; $n = 5$. (H) Levels of SREBP-1 in the nuclear fractions were determined by Western analysis and quantified by densitometry. *, $P < 0.05$ vs. Con; †, $P < 0.05$ vs. TSC2$^{-/-}$ control; $n = 5$. Values are expressed as mean ± *SEM*.

4EBP1in the presence of high glucose (Fig. 4C). It also prevented high glucose-induced ER stress response by reducing the phosphorylation of PERK and eIF2α and downregulation of GRP78 (Fig. 4D). Rapamycin treatment concomitantly reduced nuclear SREBP-1 protein levels (Fig. 4E), downregulated FAS expression (Fig. 4E), and decreased triglyceride levels (Fig. 4F), suggesting that mTORC1 mediates high glucose-induced ER stress and intracellular lipid accumulation.

To further elucidate the relationship between mTORC1 signaling and the ER stress response, we investigated whether hyperactive mTOR could increase ER stress in TSC2$^{-/-}$ MEFs, in which mTOR is constitutively activated. TSC2 deletion activated mTOR, which increased PERK and eIF2α phosphorylation and GRP78 expression. These effects were prevented by administration of rapamycin (Fig. 4G). Consistently, deletion of TSC2 increased SREBP-1 protein levels in the nuclear fractions. This increase was abolished by rapamycin treatment (Fig. 4H). These data suggest that high glucose-enhanced ER stress and lipid accumulation is mTORC1-dependent.

3.6. Activation of AMPK prevents high glucose-induced lipid accumulation by inhibiting the mTORC1-ER stress pathway

AMPK is considered a key therapeutic target for the treatment of obesity due to its role in the regulation of lipid and glucose metabolism. We therefore examined whether activation of AMPK by AICAR, a well-characterized AMPK activator, prevents high glucose-induced intracellular lipid accumulation by suppressing the mTORC1-ER stress pathway. Elevated glucose levels significantly inhibited AMPK phosphorylation at Thr172, indicating the suppression of AMPK activity (Fig. 5A). The inhibitory effect of high glucose on AMPK phosphorylation was abrogated by administration of AICAR (Fig. 5A). The restoration of AMPK activity by AICAR abolished high glucose-activated mTORC1 signaling by inhibiting mTOR phosphorylation at Ser2448 and inhibiting its downstream molecule S6K at Thr389 (Fig. 5B). Simultaneously, high glucose-stimulated ER stress response, including phosphorylation of PERK and eIF2α, and expression of GRP78 (Fig. 5C) was inhibited. Notably, the inhibition of mTORC1 and the ER stress response was

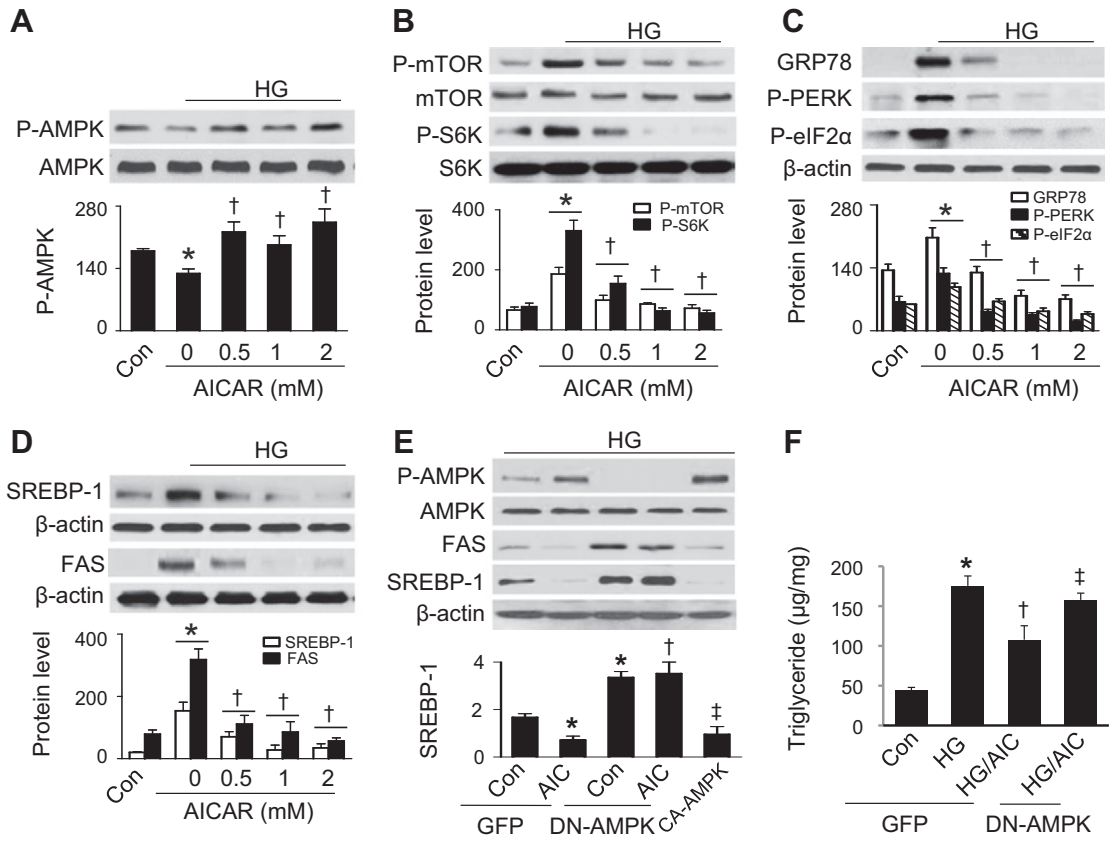

Fig. 5. AMPK activation attenuates high glucose-induced lipid accumulation through inhibition of mTORC1 signaling and ER stress. (A–D) HepG2 cells were incubated in the presence or absence of AICAR (AIC) at the indicated concentrations for 24 h. Phosphorylation of AMPK at Thr172 (A) and of mTOR and S6K (B) and expression of ER stress markers (C) were determined by Western analysis and quantitated by densitometry. *, $P < 0.05$ vs. Con; †, $P < 0.05$ vs. HG; $n = 5$. (D) Expression of SEBP-1 in the nuclear fractions and FAS in cell lysates was determined by Western analysis and quantitated by densitometry. *, $P < 0.05$ vs. Con; †, $P < 0.05$ vs. HG; $n = 5$. (E) HepG2 cells were transfected with adenovirus encoding GFP, DN-AMPK, or CA-AMPK for 48 h, and incubated in the presence or absence of 2 mM AICAR for 24 h under high glucose conditions. Levels of SREBP-1 in the nuclear fractions and expression of FAS and P-AMPK in cell lysates were determined by Western analysis. *, $P < 0.05$ vs. Con; †, $P < 0.05$ vs. GFP/AIC; ‡, $P < 0.05$ vs. DN-AMPK/AIC; $n = 5$. (F) HepG2 cells were transfected with adenovirus encoding GFP and DN-AMPK for 48 h, and incubated in the presence or absence of 2 mM AICAR and presence or absence of high glucose for 24 h. Triglyceride concentrations were measured using a commercial kit. *, $P < 0.05$ vs. Con; †, $P < 0.05$ vs. GFP/HG; ‡, $P < 0.05$ vs. GFP/HG/AIC; $n = 5$. Values are expressed as mean ± *SEM*.

associated with a reduction in nuclear SREBP-1 protein levels and downregulation of FAS protein expression (Fig. 5D).

We further determined the inhibitory effect of AMPK on high glucose-induced lipid accumulation using a genetic means. HepG2 cells were transfected with adenovirus encoding DN-AMPK, CA-AMPK, or GFP. In the presence of high glucose, AICAR treatment and transfection of CA-AMPK increased AMPK phosphorylation, while transfection of DN-AMPK had the opposite effect. Both overexpression of CA-AMPK in HepG2 cells and administration of AICAR in the cells infected with GFP adenovirus prevented high glucose-enhanced SREBP-1 protein levels in the nuclear fractions and reduced FAS expression in cell lysates (Fig. 5E). However, AICAR did not reduce FAS expression and nuclear SREBP-1 levels in the cells transfected with DN-AMPK adenovirus (Fig. 5E). In line with the alteration in nuclear SREBP-1 protein levels, AICAR treatment reduced high glucose-enhanced triglyceride contents in the cells transfected with GFP adenovirus, but the effect was absent in the cells transfected with DN-AMPK (Fig. 5F). Taken together, activation of AMPK suppressed mTROC1 signaling, leading to the inhibition of ER stress and lipid accumulation.

3.7. Chronic administration of AICAR inhibits mTORC1 and ER stress response in vivo

To determine the mechanisms underlying nutrient overload-induced hepatic lipid accumulation *in vivo*, we analyzed alteration of mTORC1 signaling, ER stress, and lipid contents in the liver in AICAR-treated and HFD-fed mice. The mice on HFD gained significantly more weight than those fed a ND (Fig. 6A). The increase in weight-gain was significantly attenuated by AICAR treatment (Fig. 6A). Total caloric intake was increased in HFD-fed mice as compared with the mice maintained on ND. Chronic administration of AICAR had no effect on caloric intake in HFD mice (Fig. 6B). Compared with ND-fed mice, HFD-fed mice exhibited a reduction in AMPK phosphorylation, suggesting an inhibition of AMPK. AMPK activity was restored by chronic AICAR treatment (Fig. 6C). HFD feeding resulted in activation of mTORC1 signaling, as determined by an increase in S6K phosphorylation (Fig. 6D). This triggered the ER stress response by increasing the phosphorylation of PERK and eIF2α (Fig. 6E), all of which were attenuated by AICAR treatment (Fig. 6C and E). Notably, HFD-enhanced nuclear SREBP-1 levels were abrogated by chronic administration of AICAR (Fig. 6F).

3.8. AICAR treatment prevents hepatic lipid accumulation and insulin resistance

We next investigated whether AMPK activation prevents nutrient overload-induced hepatic lipid accumulation and insulin resistance *in vivo*. Consistent with the activation of SREBP-1, HFD-fed mice exhibited upregulation of SREBP-1 target genes FAS and ACC1 (Fig. 7A). This was in turn associated with more fat deposition in the liver and viscera (Fig. 7B), increases in subcutaneous and visceral fat mass (Fig. 7C), and higher levels of triglycerides and cholesterol in the

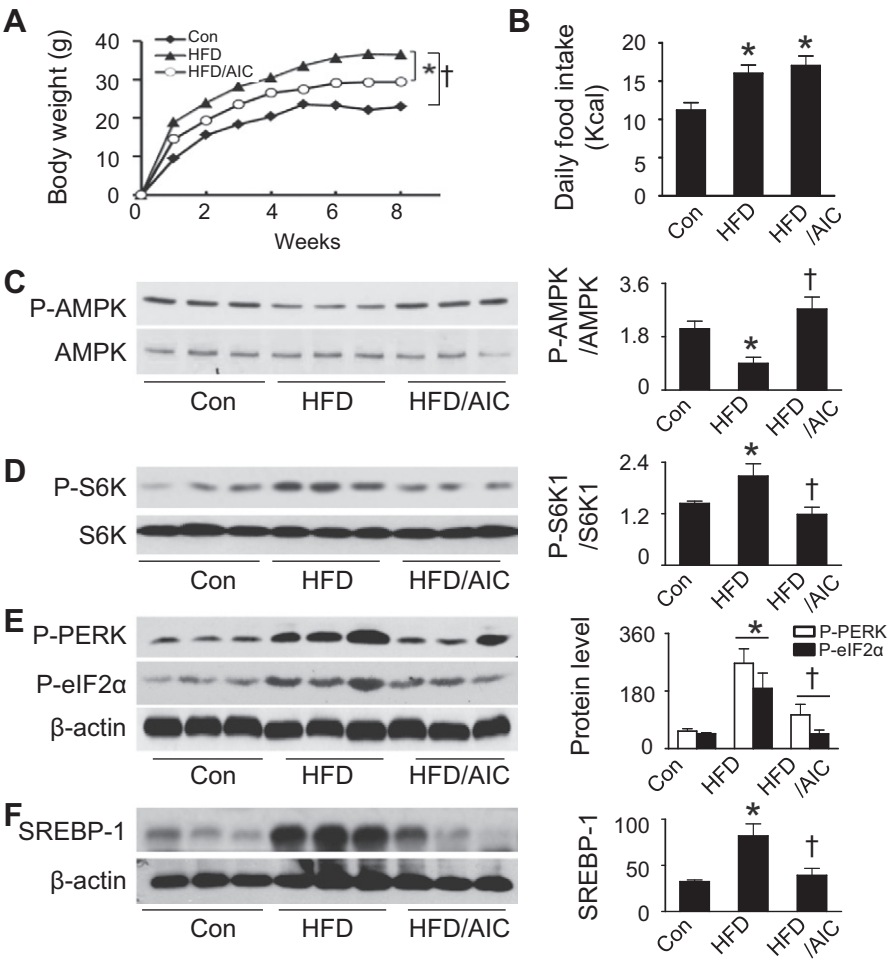

Fig. 6. AMPK activation attenuates HFD-stimulated mTORC1 signaling and ER stress *in vivo*. Mice were fed a normal diet (Con) or HFD and treated with AICAR (AIC) or vehicle. (A) Body weights were monitored at the weeks indicated. $n = 6$; *, $P < 0.05$ vs. HFD; †, $P < 0.05$ vs. ND. (B) Daily caloric intake was calculated from the amount of ingested food in individually-caged mice. $n = 6$; *, $P < 0.05$ vs. Con. Phosphorylation of AMPK (C) ($n = 6$) and S6K (D) ($n = 6$) and protein levels of ER stress markers P-PERK and P-eIF2α (E) ($n = 5$) in liver homogenates were determined by Western analysis and quantified by densitometry. (F) Protein levels of SREBP-1 in the nuclear fractions were measured by Western blotting ($n = 5$) *, $P < 0.05$ vs. Con; †, $P < 0.05$ vs. HFD. Values are expressed as mean ± *SEM*.

liver (Fig. 7D and E). All these effects were abrogated by chronic administration of AICAR (Fig. 7A–E). To determine the effect of AICAR on insulin signaling, we first examined the effect of AICAR on fasting glucose levels. We found that chronic administration of AICAR normalized fasting blood glucose in HFD-fed mice (Fig. 7F). We next performed a hyperinsulinemic–euglycemic clamp study in these mice. Consistent with the fact that diet-induced obesity inhibits insulin sensitivity, we observed a significant decrease in the glucose infusion rate in HFD-fed mice (Fig. 7G and H). The glucose infusion rate in AICAR-treated and HFD-fed mice was significantly higher than that in HFD-fed mice (Fig. 7G and H), indicating that chronic administration of AICAR enhances insulin sensitivity in a diet-induced obesity model.

4. Discussion

Excessive intake of nutrients is a major cause of lipid accumulation, which leads to the development of obesity and insulin resistance. Thus, identification of the mechanistic link between nutrient overload and lipid accumulation might help to define novel nutritional and pharmacological approaches for the treatment of obesity and insulin resistance. The present study demonstrated that excess nutrients triggered the ER stress response, activated SREBP-1, and increased intracellular lipid levels. All of these were abolished by inhibiting the mTORC1 signaling pathway. Activation of AMPK prevented high glucose-activated mTORC1 signaling, leading to suppression of the ER stress response and lipid accumulation. Moreover, treatment of HFD-fed mice with AICAR inhibited the mTORC1 pathway, suppressed the ER stress response, and prevented insulin resistance and hepatic lipid accumulation. These findings establish a novel and attractive model that suppression of mTORC1 by AMPK inhibits nutrient overload-induced ER stress, which in turn prevents hepatic lipid accumulation and insulin resistance (Fig. 7I).

Under nutrient overload conditions, increased phosphorylation of PERK and eIF2α is associated with upregulation of SREBP-1 and lipid accumulation. Gene silencing of eIF2α abolishes lipid accumulation induced by elevated excess nutrients, suggesting that the PERK/eIF2α UPR branch serves as a critical regulator of lipid metabolism via regulation of SREBP1 processing and target gene expression. PERK is a major transducer of the ER stress response and it can directly phosphorylate eIF2α [42,43]. Phosphorylated eIF2α specifically promotes the translation of activating transcription factor 4, a member of the cAMP-response element-binding protein family, which activates SREBP1 [44] and upregulates the genes related to lipogenesis. In support of this model, recent studies demonstrate that PERK knockout substantially decreases SREBP-1 activity and reduces lipogenesis in mammary glands [4]. Dephosphorylation of eIF2α diminishes hepatosteatosis in HFD-fed animals [45]. These studies link the PERK/eIF2α UPR branch to the development of dyslipidemia. However, other groups reported that feeding a high-sucrose diet results in hepatosteatosis and activation of the IRE1α-XBP1 branch in the liver [46]. A single high-carbohydrate

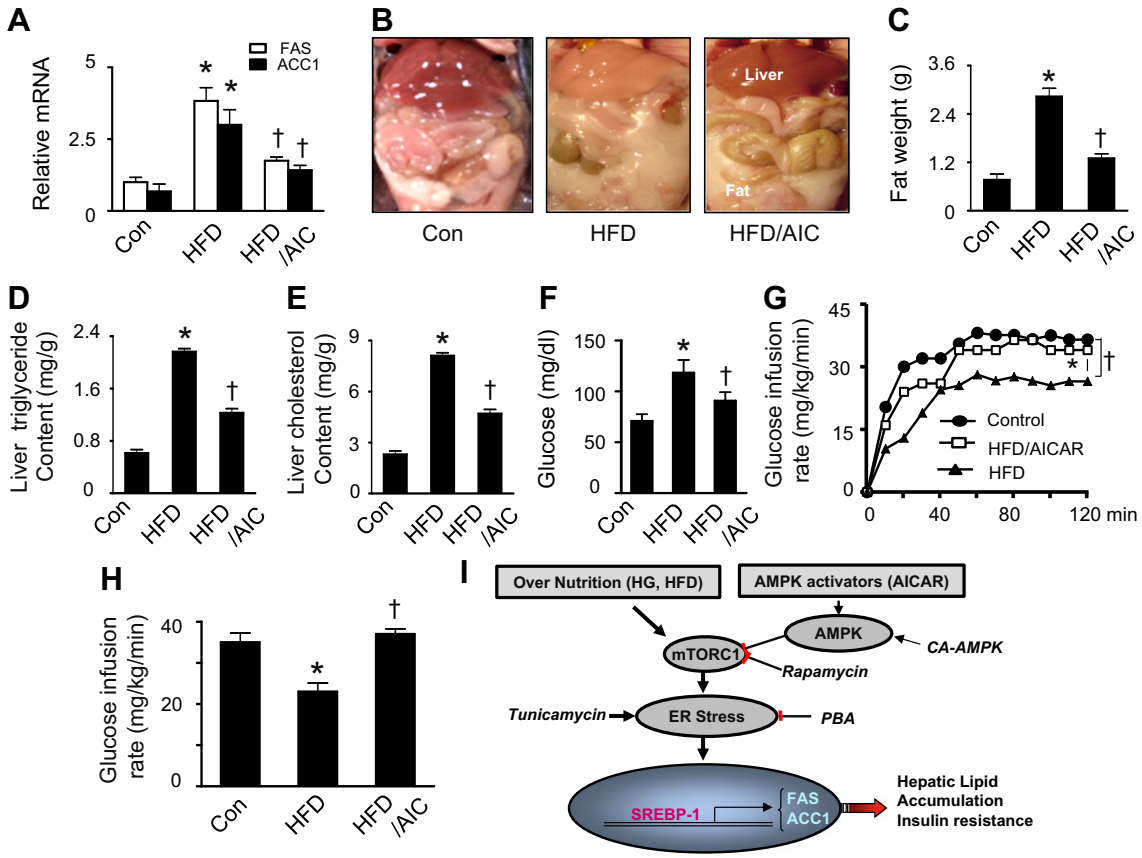

Fig. 7. Activation of AMPK reduces HFD-induced lipid accumulation and improves insulin sensitivity *in vivo*. Mice were fed a normal diet (Con) or HFD and treated with AICAR (AIC) or vehicle. (A) Relative levels of FAS and ACC1 mRNA in liver were determined by Q RT-PCR. *, $P < 0.05$ vs. Con; †, $P < 0.05$ vs. HFD; $n = 6$. (B) Representative images showing increased hepatic and visceral fat; $n = 5$ for each group. (C) Total fat mass was measured after the treatment. *, $P < 0.05$ vs. Con; †, $P < 0.05$ vs. HFD; $n = 6$. (D and E) Liver lipids were extracted and hepatic triglyceride and cholesterol levels were assayed using a commercial kit. *, $P < 0.05$ vs. Con; †, $P < 0.05$ vs. HFD; $n = 6$. (F) Fasting blood glucose levels were measured in tail vein blood samples using a glucometer. *, $P < 0.05$ vs. Con; †, $P < 0.05$ vs. HFD; $n = 6$. (G and H) Hyperinsulinemic–euglycemic clamps were performed over a 120-min period. Insulin sensitivity was evaluated based on average glucose infusion rate at equilibrium in a hyperinsulinemic–euglycemic clamp (3 mU insulin/kg/min). *, $P < 0.05$ vs. Con; †, $P < 0.05$ vs. HFD; $n = 5$. Values are expressed as mean ± *SEM*. (I) Proposed mechanism by which AMPK inhibits excess nutrient-induced lipid accumulation. Excess nutrients stimulate mTORC1 signaling, which activates ER stress, leading to activation of SREBP-1 and consequent lipid accumulation. Activation of AMPK prevents lipid accumulation by suppression of the mTORC1-ER stress pathway.

meal also results in the phosphorylation of IRE1α, induces XBP1 splicing, and increases expression of lipogenic genes in the liver [47]. Although XBP1 is identified as an important regulator of hepatic lipogenesis in carbohydrate-fed mice, its function in regulating lipogenesis is independent of the ER stress response [48]. Thus, further investigations are needed to determine whether other UPR branches are involved in the regulation of hepatic lipogenesis under excess nutrient conditions.

The mTORC1 signaling pathway integrates inputs from several upstream pathways, including the nutrient-sensing pathway, with cell growth and metabolism. These conditions may also challenge ER integrity, evoking the UPR. Consistent with a previous finding that knockout of TSC1 or TSC2 triggers the UPR, resulting in mTOR-mediated feedback inhibition of insulin action and increased apoptosis [13], we observed that nutrient overload causes ER stress and activates the UPR in an mTORC1-dependent manner. These results suggest that activation of the UPR pathway is an important consequence of mTORC1 activation, and contributes to the development of insulin resistance. Conversely, as an intermediary of insulin signaling, mTORC1 can also be activated by ER stress [49]. Previous studies have shown that downstream effector of mTOR, S6K, contributes to the development of insulin resistance in a condition of energy surplus by negatively regulating insulin receptor substrate 1 function [50]. Thus, under conditions of nutrient overload, the mTORC1-S6K1 axis and UPR might coordinately regulate insulin signaling, resulting in inhibition of insulin sensitivity. As insulin is a major stimulus for many biosynthetic pathways, including protein synthesis, the feedback inhibition of insulin action in the presence of ER stress may represent an adaptive response that protects the cells from further aberrant protein synthesis and stress in the ER by partially blocking protein translation and insulin responsiveness.

Another important set of findings is that activation of AMPK downregulates mTORC1 activity, attenuates the UPR, reduces lipid accumulation, and enhances insulin sensitivity *in vivo*. Under excess nutrient conditions, two important signaling pathways in sensing nutrient and energy status, AMPK and mTORC1, coordinately regulate the UPR, lipid metabolism, and insulin signaling. AMPK has been reported to inhibit mTORC1 either through direct phosphorylation of mTOR [51] or through phosphorylation and activation of tuberin [52]. In HepG2 cells exposed to high glucose, inactivation of AMPK activates the mTORC1 signaling pathway, leading to lipid accumulation and suppression of insulin signaling. Administration of AICAR restores AMPK activity, inhibits mTORC1 signaling, reduces lipid accumulation, and improves insulin sensitivity. These results are consistent with the observation that activation of AMPK by AICAR inhibits the phosphorylation of S6K and reduces its activity in SV40-immortalized human corneal epithelial cells [53]. In addition, under energy depletion conditions, AMPK phosphorylates TSC2 and enhances its activity, which inhibits mTORC1 signaling, protecting cells from energy deprivation-induced apoptosis [54]. Taken together, AMPK protects against ER stress and lipid accumulation through the inhibition of mTORC1 signaling. This conclusion is also supported by our *in vivo* observation that activation of AMPK by chronic administration of

AICAR reduced S6K phosphorylation, inhibited the ER stress response, and attenuated hepatic lipid accumulation and insulin resistance.

In summary, activation of AMPK prevents hepatic lipid accumulation and insulin resistance induced by excess nutrients. This effect could be mediated by AMPK suppression of mTORC1 and UPR signaling. These findings highlight the importance of the AMPK–mTORC1 axis in the regulation of UPR under nutritional overload conditions, and provide new insights into the mechanism by which AMPK activation prevents hepatic lipid accumulation and insulin resistance. These studies also suggest that either activation of AMPK or inhibition of mTORC1 and UPR may have potential for the treatment of chronic metabolic diseases, including obesity, type 2 diabetes, and cardiovascular disease.

Disclosure statement

No conflicts of interest relevant to this article are reported.

Acknowledgements

We thank Ms. Kathy Kyler, the University of Oklahoma Health Sciences Center, for her help in editing the manuscript. This study was supported by funding from the following: NIH (HL079584, HL080499, HL074399, HL089920, and HL096032 to M.Z., and 1P20RR024215-01 to Z.X. and M.Z.), the American Heart Association Scientist Development Grant (Z.X.), the Juvenile Diabetes Research Foundation (M.Z.), Oklahoma Center for the Advancement of Science and Technology (M.Z. and Z.X.), and the American Diabetes Association (M.Z.). Dr. M.H. Zou is a recipient of the National Established Investigator Award of American Heart Association.

References

[1] S. Fu, S.M. Watkins, G.S. Hotamisligil, The role of endoplasmic reticulum in hepatic lipid homeostasis and stress signaling, Cell Metab. 15 (2012) 623–634.
[2] Y. Dong, M. Zhang, B. Liang, Z. Xie, Z. Zhao, S. Asfa, H.C. Choi, M.H. Zou, Reduction of AMP-activated protein kinase alpha2 increases endoplasmic reticulum stress and atherosclerosis in vivo, Circulation 121 (2010) 792–803.
[3] S.M. Colgan, D. Tang, G.H. Werstuck, R.C. Austin, Endoplasmic reticulum stress causes the activation of sterol regulatory element binding protein-2, Int. J. Biochem. Cell Biol. 39 (2007) 1843–1851.
[4] E. Bobrovnikova-Marjon, G. Hatzivassiliou, C. Grigoriadou, M. Romero, D.R. Cavener, C.B. Thompson, J.A. Diehl, PERK-dependent regulation of lipogenesis during mouse mammary gland development and adipocyte differentiation, Proc. Natl. Acad. Sci. U. S. A. 105 (2008) 16314–16319.
[5] S.H. Um, D. D'Alessio, G. Thomas, Nutrient overload, insulin resistance, and ribosomal protein S6 kinase 1, S6K1, Cell Metab. 3 (2006) 393–402.
[6] K. Hara, Y. Maruki, X. Long, K. Yoshino, N. Oshiro, S. Hidayat, C. Tokunaga, J. Avruch, K. Yonezawa, Raptor, a binding partner of target of rapamycin (TOR), mediates TOR action, Cell 110 (2002) 177–189.
[7] D.H. Kim, D.D. Sarbassov, S.M. Ali, J.E. King, R.R. Latek, H. Erdjument-Bromage, P. Tempst, D.M. Sabatini, mTOR interacts with raptor to form a nutrient-sensitive complex that signals to the cell growth machinery, Cell 110 (2002) 163–175.
[8] E. Jacinto, R. Loewith, A. Schmidt, S. Lin, M.A. Ruegg, A. Hall, M.N. Hall, Mammalian TOR complex 2 controls the actin cytoskeleton and is rapamycin insensitive, Nat. Cell Biol. 6 (2004) 1122–1128.
[9] D.D. Sarbassov, S.M. Ali, D.H. Kim, D.A. Guertin, R.R. Latek, H. Erdjument-Bromage, P. Tempst, D.M. Sabatini, Rictor, a novel binding partner of mTOR, defines a rapamycin-insensitive and raptor-independent pathway that regulates the cytoskeleton, Curr. Biol. 14 (2004) 1296–1302.
[10] P. Kapahi, D. Chen, A.N. Rogers, S.D. Katewa, P.W. Li, E.L. Thomas, L. Kockel, With TOR, less is more: a key role for the conserved nutrient-sensing TOR pathway in aging, Cell Metab. 11 (2010) 453–465.
[11] T.R. Peterson, S.S. Sengupta, T.E. Harris, A.E. Carmack, S.A. Kang, E. Balderas, D.A. Guertin, K.L. Madden, A.E. Carpenter, B.N. Finck, D.M. Sabatini, mTOR complex 1 regulates lipin 1 localization to control the SREBP pathway, Cell 146 (2011) 408–420.
[12] J.L. Yecies, H.H. Zhang, S. Menon, S. Liu, D. Yecies, A.I. Lipovsky, C. Gorgun, D.J. Kwiatkowski, G.S. Hotamisligil, C.H. Lee, B.D. Manning, Akt stimulates hepatic SREBP1c and lipogenesis through parallel mTORC1-dependent and independent pathways, Cell Metab. 14 (2011) 21–32.
[13] U. Ozcan, L. Ozcan, E. Yilmaz, K. Duvel, M. Sahin, B.D. Manning, G.S. Hotamisligil, Loss of the tuberous sclerosis complex tumor suppressors triggers the unfolded protein response to regulate insulin signaling and apoptosis, Mol. Cell 29 (2008) 541–551.
[14] D.G. Hardie, Minireview: the AMP-activated protein kinase cascade: the key sensor of cellular energy status, Endocrinology 144 (2003) 5179–5183.
[15] D. Carling, The AMP-activated protein kinase cascade–a unifying system for energy control, Trends Biochem. Sci. 29 (2004) 18–24.
[16] D.G. Hardie, J.W. Scott, D.A. Pan, E.R. Hudson, Management of cellular energy by the AMP-activated protein kinase system, FEBS Lett. 546 (2003) 113–120.
[17] K. Terai, Y. Hiramoto, M. Masaki, S. Sugiyama, T. Kuroda, M. Hori, I. Kawase, H. Hirota, AMP-activated protein kinase protects cardiomyocytes against hypoxic injury through attenuation of endoplasmic reticulum stress, Mol. Cell. Biol. 25 (2005) 9554–9575.
[18] Z. Xie, Y. Dong, M. Zhang, M.Z. Cui, R.A. Cohen, U. Riek, D. Neumann, U. Schlattner, M. H. Zou, Activation of protein kinase C zeta by peroxynitrite regulates LKB1-dependent AMP-activated protein kinase in cultured endothelial cells, J. Biol. Chem. 281 (2006) 6366–6375.
[19] Z. Xie, Y. Dong, R. Scholz, D. Neumann, M.H. Zou, Phosphorylation of LKB1 at serine 428 by protein kinase C-zeta is required for metformin-enhanced activation of the AMP-activated protein kinase in endothelial cells, Circulation 117 (2008) 952–962.
[20] J.M. Cacicedo, M.S. Gauthier, N.K. Lebrasseur, R. Jasuja, N.B. Ruderman, Y. Ido, Acute exercise activates AMPK and eNOS in the mouse aorta, Am. J. Physiol. Heart Circ. Physiol. 301 (2011) H1255–H1265.
[21] N. Taleux, I. P. De, C. Deransart, G. Lacraz, R. Favier, X.M. Leverve, L. Hue, B. Guigas, Lack of starvation-induced activation of AMP-activated protein kinase in the hypothalamus of the Lou/C rats resistant to obesity, Int. J. Obes. (Lond.) 32 (2008) 639–647.
[22] Z. Xie, C. He, M.H. Zou, AMP-activated protein kinase modulates cardiac autophagy in diabetic cardiomyopathy, Autophagy 7 (2011) 1254–1255.
[23] C. He, H. Zhu, H. Li, M.H. Zou, Z. Xie, Dissociation of Bcl-2-Beclin1 complex by activated AMPK enhances cardiac autophagy and protects against cardiomyocyte apoptosis in diabetes, Diabetes 62 (2013) 1270–1281.
[24] C. Ouyang, J. You, Z. Xie, The interplay between autophagy and apoptosis in the diabetic heart, J. Mol. Cell. Cardiol. 71C (2014) 71–80.
[25] Z. Xie, K. Lau, B. Eby, P. Lozano, C. He, B. Pennington, H. Li, S. Rathi, Y. Dong, R. Tian, D. Kem, M.H. Zou, Improvement of cardiac functions by chronic metformin treatment is associated with enhanced cardiac autophagy in diabetic OVE26 mice, Diabetes 60 (2011) 1770–1778.
[26] M.H. Zou, Z. Xie, Regulation of interplay between autophagy and apoptosis in the diabetic heart: new role of AMPK, Autophagy 9 (2013) 624–625.
[27] B.J. Davis, Z. Xie, B. Viollet, M.H. Zou, Activation of the AMP-activated kinase by antidiabetes drug metformin stimulates nitric oxide synthesis in vivo by promoting the association of heat shock protein 90 and endothelial nitric oxide synthase, Diabetes 55 (2006) 496–505.
[28] Z. Xie, Y. Dong, J. Zhang, R. Scholz, D. Neumann, M.H. Zou, Identification of the serine 307 of LKB1 as a novel phosphorylation site essential for its nucleocytoplasmic transport and endothelial cell angiogenesis, Mol. Cell. Biol. 29 (2009) 3582–3596.
[29] H. Li, M. Xu, J. Lee, C. He, Z. Xie, Leucine supplementation increases SIRT1 expression and prevents mitochondrial dysfunction and metabolic disorders in high-fat diet-induced obese mice, Am. J. Physiol. Endocrinol. Metab. 303 (2012) E1234–E1244.
[30] T.T. Tran, N. Gupta, T. Goh, D. Naigamwalla, M.C. Chia, N. Koohestani, S. Mehrotra, G. McKeown-Eyssen, A. Giacca, W.R. Bruce, Direct measure of insulin sensitivity with the hyperinsulinemic–euglycemic clamp and surrogate measures of insulin sensitivity with the oral glucose tolerance test: correlations with aberrant crypt foci promotion in rats, Cancer Epidemiol. Biomarkers Prev. 12 (2003) 47–56.
[31] J. Folch, M. Lees, G.H. Sloane Stanley, A simple method for the isolation and purification of total lipides from animal tissues, J. Biol. Chem. 226 (1957) 497–509.
[32] C. He, H. Zhu, W. Zhang, I. Okon, Q. Wang, H. Li, Y.Z. Le, Z. Xie, 7-Ketocholesterol induces autophagy in vascular smooth muscle cells through Nox4 and Atg4B, Am. J. Pathol. 183 (2013) 626–637.
[33] Z. Xie, J. Zhang, J. Wu, B. Viollet, M.H. Zou, Upregulation of mitochondrial uncoupling protein-2 by the AMP-activated protein kinase in endothelial cells attenuates oxidative stress in diabetes, Diabetes 57 (2008) 3222–3230.
[34] L. Tedesco, A. Valerio, C. Cervino, A. Cardile, C. Pagano, R. Vettor, R. Pasquali, M.O. Carruba, G. Marsicano, B. Lutz, U. Pagotto, E. Nisoli, Cannabinoid type 1 receptor blockade promotes mitochondrial biogenesis through endothelial nitric oxide synthase expression in white adipocytes, Diabetes 57 (2008) 2028–2036.
[35] H. Li, J. Lee, C. He, M.H. Zou, Z. Xie, Suppression of the mTORC1/STAT3/Notch1 pathway by activated AMPK prevents hepatic insulin resistance induced by excess amino acids, Am. J. Physiol. Endocrinol. Metab. 306 (2014) E197–E209.
[36] M.W. Pfaffl, A new mathematical model for relative quantification in real-time RT-PCR, Nucleic Acids Res. 29 (2001) e45.
[37] I. Shimomura, Y. Bashmakov, J.D. Horton, Increased levels of nuclear SREBP-1c associated with fatty livers in two mouse models of diabetes mellitus, J. Biol. Chem. 274 (1999) 30028–30032.
[38] I. Shimomura, M. Matsuda, R.E. Hammer, Y. Bashmakov, M.S. Brown, J.L. Goldstein, Decreased IRS-2 and increased SREBP-1c lead to mixed insulin resistance and sensitivity in livers of lipodystrophic and ob/ob mice, Mol. Cell 6 (2000) 77–86.
[39] C. Han, M.K. Nam, H.J. Park, Y.M. Seong, S. Kang, H. Rhim, Tunicamycin-induced ER stress upregulates the expression of mitochondrial HtrA2 and promotes apoptosis through the cytosolic release of HtrA2, J. Microbiol. Biotechnol. 18 (2008) 1197–1202.
[40] U. Ozcan, E. Yilmaz, L. Ozcan, M. Furuhashi, E. Vaillancourt, R.O. Smith, C.Z. Gorgun, G.S. Hotamisligil, Chemical chaperones reduce ER stress and restore glucose homeostasis in a mouse model of type 2 diabetes, Science 313 (2006) 1137–1140.
[41] N. Hay, N. Sonenberg, Upstream and downstream of mTOR, Genes Dev. 18 (2004) 1926–1945.
[42] R.J. Kaufman, Stress signaling from the lumen of the endoplasmic reticulum: coordination of gene transcriptional and translational controls, Genes Dev. 13 (1999) 1211–1233.
[43] R.C. Wek, H.Y. Jiang, T.G. Anthony, Coping with stress: eIF2 kinases and translational control, Biochem. Soc. Trans. 34 (2006) 7–11.

[44] L. Zhou, Y. Li, T. Nie, S. Feng, J. Yuan, H. Chen, Z. Yang, Clenbuterol inhibits SREBP-1c expression by activating CREB1, J. Biochem. Mol. Biol. 40 (2007) 525–531.
[45] S. Oyadomari, H.P. Harding, Y. Zhang, M. Oyadomari, D. Ron, Dephosphorylation of translation initiation factor 2alpha enhances glucose tolerance and attenuates hepatosteatosis in mice, Cell Metab. 7 (2008) 520–532.
[46] D. Wang, Y. Wei, M.J. Pagliassotti, Saturated fatty acids promote endoplasmic reticulum stress and liver injury in rats with hepatic steatosis, Endocrinology 147 (2006) 943–951.
[47] K.T. Pfaffenbach, A.M. Nivala, L. Reese, F. Ellis, D. Wang, Y. Wei, M.J. Pagliassotti, Rapamycin inhibits postprandial-mediated X-box-binding protein-1 splicing in rat liver, J. Nutr. 140 (2010) 879–884.
[48] A.H. Lee, E.F. Scapa, D.E. Cohen, L.H. Glimcher, Regulation of hepatic lipogenesis by the transcription factor XBP1, Science 320 (2008) 1492–1496.
[49] M. Flamment, E. Hajduch, P. Ferre, F. Foufelle, New insights into ER stress-induced insulin resistance, Trends Endocrinol. Metab. 23 (2012) 381–390.
[50] Y. Zick, Uncoupling insulin signalling by serine/threonine phosphorylation: a molecular basis for insulin resistance, Biochem. Soc. Trans. 32 (2004) 812–816.
[51] S.W. Cheng, L.G. Fryer, D. Carling, P.R. Shepherd, Thr2446 is a novel mammalian target of rapamycin (mTOR) phosphorylation site regulated by nutrient status, J. Biol. Chem. 279 (2004) 15719–15722.
[52] K. Inoki, Y. Li, T. Zhu, J. Wu, K.L. Guan, TSC2 is phosphorylated and inhibited by Akt and suppresses mTOR signalling, Nat. Cell Biol. 4 (2002) 648–657.
[53] N. Kimura, C. Tokunaga, S. Dalal, C. Richardson, K. Yoshino, K. Hara, B.E. Kemp, L.A. Witters, O. Mimura, K. Yonezawa, A possible linkage between AMP-activated protein kinase (AMPK) and mammalian target of rapamycin (mTOR) signalling pathway, Genes Cells 8 (2003) 65–79.
[54] K. Inoki, T. Zhu, K.L. Guan, TSC2 mediates cellular energy response to control cell growth and survival, Cell 115 (2003) 577–590.